Dynamics of Wormlike Polymers in Solution: Self-Diffusion and Zero-Shear Viscosity

G. Petekidis,* D. Vlassopoulos, and G. Fytas

Institute of Electronic Structure and Laser, Foundation for Research and Technology-Hellas, P.O. Box 1527, 711 10 Heraklion, Crete, Greece

G. Fleischer

Fakultät für Physik und Geowissenschaften, Universität Leipzig, Linnerstrasse 5, D-04103 Leipzig, Germany

G. Wegner

Max-Planck Institut für Polymerforschung, P.O. Box 3148, 55021 Mainz, Germany

Received June 2, 2000

ABSTRACT: The dynamics of hairy-rod poly(*p*-phenylene)s in isotropic solutions are investigated by pulse field gradient NMR (PFG−NMR) and dynamic shear rheology for four different contour lengths over a broad concentration range. The self-diffusion coefficient, measured directly by PFG−NMR, and the longest relaxation time, determined by rheology, exhibit a significant slowing down with concentration, while the zero-shear viscosity increases. These dependencies are described successfully by predictions according to the fuzzy cylinder model and the "hole theory" considering the effect of the intermolecular hydrodynamic interactions. The entanglement effects are found to be stronger in the rotational motion and the zero-shear viscosity than in the translational motion and moreover to increase for shorter, more rodlike chains. The self-friction coefficient determined from PFG−NMR is found to differ from the cooperative friction measured by dynamic light scattering.

I. Introduction

It is well-known that a thorough understanding of the dynamics of polymers in solution requires the systematic study of the main transport properties, namely the center of mass self-diffusion and the rotational and the cooperative diffusion, as well as the zero shear viscosity. This is especially true in the case of the less well-studied semiflexible polymers where because of the persistence and anisotropy of shape additional parameters for describing conformation and mobility are introduced. In two previous investigations,[1] we have studied the orientation dynamics and the cooperative diffusion of isotropic solutions of hairy-rod poly(*p*-phenylenes) with aromatic sulfonated side chains (PPPS, see Chart 1) in a wide range of concentrations. The pertinent findings regarding the orientation dynamics studied by depolarized dynamic light scattering relate to the collective rotational motion of the Kuhn segments of the semiflexible chains and the cooperative motion of orientationally correlated segment pairs.[1a] Referring to the diffusion dynamics, we presented a detailed investigation of the polarized dynamic structure factor of the same polymers in solution measured by polarized dynamic light scattering, to quantify the relaxation of concentration fluctuations through the mechanism of cooperative diffusion, in particular in the concentrated isotropic regime.[1b] The present study complements the previous, and together they provide necessary ingredients for understanding the physics governing the solution dynamics of semiflexible polymers. The PPPS molecules are a new class of polymers with potential technological applications which moreover may be considered as good model semiflexible polymers with high optical anisotropy, well characterized structure and good solubility in various solvents, thus allowing exploring their transport properties over a wide concentration range.

Chart 1. Poly(*p*-phenylene) with Aromatic Sulfonate Side Groups (PPPS)

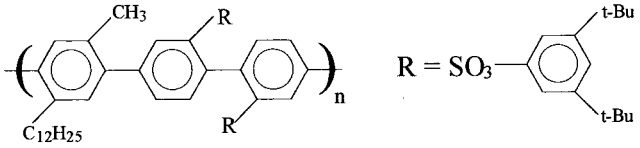

The single-particle, incoherent, structure factor was determined using PFG−NMR data while dynamic shear rheology was utilized to measure the dynamic storage (G') and loss (G'') moduli and the complex shear viscosity of the polymer solution. The former experimental technique yields the self-diffusion coefficient and the latter the zero-shear viscosity and the longest relaxation time. As in the previous work,[1] this study provides dynamic information in the isotropic regime up to very high concentrations (about 50 wt %), due to the fact that these stiff PPPS polymers do not exhibit an isotropic to nematic transition.

The translational self-diffusion coefficient D_s of a polymer in solution can be measured by techniques probing the single-particle motion such as forced Rayleigh scattering (FRS), fringe pattern recovery after photobleaching (FRAP) and PFG−NMR, in addition to computer simulations. The experimental studies of the self-diffusion in isotropic solutions of stiff polymers involve FRS and FRAP measurements of biological polymers like xanthan (a stiff double-helical polysac-

* Corresponding author. Present address: Department of Physics and Astronomy, University of Edinburgh, JCMB, The Kings Buildings, Mayfield Road, Edinburgh EH9 3JZ,U.K.

10.1021/ma000976w CCC: $19.00
Published on Web 12/26/2000

charide)[2] and DNA[3] or synthetic polymers like poly(γ-benzyl-L-glutamate) (PBLG).[4] Whereas all these early studies revealed a decrease of the D_s with concentration, a quantitative description of the data according to a theoretical model was either absent or inconclusive. Such an analysis has been presented for the long-time translational self-diffusion of colloidal rods measured in both isotropic and nematic solutions by FRAP.[5] A theoretical description of both translational and rotational diffusivities as well as the zero-shear viscosity of stiff polymers in solution has been presented by Sato et al.[6,7] based on the "fuzzy cylinder" model. This model has been successfully used to describe the viscosity data of a wide range of stiff macromolecules including aqueous xanthan solutions[8] and solutions of PHIC;[9,10] very recently, it was also used to predict the self-diffusion coefficient deduced from the mutual diffusion coefficient in solutions of PHIC.[10] The latter was based on the assumption that the friction coefficient involved in the cooperative diffusion coefficient is the same with the one involved in the self-diffusion, an assumption that is both experimentally[1b,4] and theoretically[11] questionable.

In view of the above, the need for a complete self-consistent set of independent experimental measurements of the key transport properties in different semiflexible polymers is evident. Thus, the scope of this paper is to present such a set of careful experimental data on the self-diffusion, the longest relaxation time, and the zero-shear viscosity of PPPS with aromatic sulfonated side groups in a broad concentration regime and critically compare them with the current theoretical models.[7] The target is to describe all properties in a self-consistent manner and in this process identify the potential aspects of the theory that need being reconsidered. The paper is organized as follows: Section II provides a concise review of the relevant theoretical approaches necessary for the subsequent quantitative analysis of the experimental data as well as a summary of relevant experiments studies. Section III contains the experimental information while the results are presented and discussed in section IV, and the main conclusions are summarized in section V.

II. Theoretical Background

In all theoretical approaches, the transport properties of stiff polymer chains in dilute solutions are related, with the flexibility parameter of the chain, i.e., the persistence length l.[12] In the dilute limit, where the chains move without any interactions, Yamakawa and Fujii[13] calculated the translational diffusion coefficient in the framework of the wormlike model[14] to be of the form

$$D_0 = \frac{k_B T}{3\pi\eta_s L} F(L/2l, b/2l) \qquad (1)$$

where L is the contour length of the polymer chain, b its diameter, η_s the solvent viscosity and F a function of the ratios of the contour length, and the diameter to the persistence length, which involves corrections and end effects and is given in two different functional forms, depending on whether the ratio L/l is larger or smaller than 2.278.

The dynamics in the semidilute and concentrated regions are largely affected by intermolecular interactions, which are negligible in the dilute region. The first theory for the dynamics of nondilute solutions of rigid rods was presented by Doi and Edwards (DE).[15] They used the tube concept to describe the dynamics of nondilute solutions of rods and assuming a free axial diffusion ($D_{||} = D_{||,0}$) and a frozen diffusion perpendicular to the rod axes ($D_\perp = 0$) they predicted that the translational diffusion of a rod decreases to half of its dilute value ($D_s = D_0/2$, using $D_{||,0} = 2D_{\perp,0}$), and it becomes concentration independent in the semidilute region. In this theory, the effects of finite diameter, molecular flexibility, and hydrodynamic interactions were not considered. The refinements of the DE theory concerning the self-diffusion relate to the introduction of finite thickness and flexibility effects. Edwards and Evans[16a] used a mean field theory to calculate the slowing down of the self-diffusion while Edwards and Vilgis[16b] introduced cooperative effects in the motion of long rods in highly concentrated solution in an effort to describe the dynamics of the glass transition. Latter, Teraoka and Hayakawa[17] calculated the decrease of the lateral diffusion, whereas an extension of the Edwards–Evans model to a wider concentration range was achieved by Sato and Teramoto.[7,18]

The flexibility can affect the dynamic behavior and very often deviations between experiments and theory of rods are attributed to it. The dynamics of semiflexible chains in nondilute solutions have been studied in the framework of two models: the reptation model for a wormlike chain[19] and the "fuzzy cylinder" model.[6,7] Whereas the former predicts a concentration independent self-diffusion in the concentrated regime, the latter predicts a behavior similar to that of rodlike chains with renormalized dimensions L_e and b_e. The basic assumption of the "fuzzy cylinder" model is that the changes of the local conformation of the stiff polymer chain are much faster than its overall translational and rotational motion; consequently, the global motion of the chain can be identified with that of a distribution of segments with cylindrical symmetry represented by the fuzzy cylinder. The latter has an effective length $L_e = \langle R^2\rangle^{1/2}$ and diameter $b_e = (\langle H^2\rangle + b^2)^{1/2}$, where $\langle R^2\rangle$ is the mean square end-to-end distance and $\langle H^2\rangle$ is the mean square distance between the chain midpoint and the end-to-end axis.

Both the transverse and the longitudinal diffusion coefficients can be treated by a mean-field Green function method.[7] Accordingly, the perpendicular diffusion coefficient in the fuzzy cylinder model reads

$$\frac{D_\perp}{D_{\perp,0}} = \left(1 + \beta_\perp^{-1/2} L_e^{3} \rho f_\perp(b_e/L_e)\sqrt{2C\frac{D_{||,0}}{D_{||}}}\right)^{-2} \qquad (2)$$

where ρ is the number density, $C = D_{\perp,0}/D_{||,0}$ is the ratio of the transverse to the longitudinal self-diffusion coefficient at the zero concentration limit, $\beta_\perp$ is a constant and $f_\perp(b_e/L_e) = (1 + C_\perp b_e/3L_e)(1 + C_\perp b_e/L_e)$ is a function of the aspect ratio L_e/b_e with $0 < C_\perp < 1$ depending on how effective the mechanism of segment fluctuation is in releasing a test chain hindered by its neighbors. Teraoka[7] used the cage model to calculate the probability of entanglement for infinitely thin rods and found $\beta_\perp = 561$. As can be seen from eq 2, in order to determine the concentration dependence of the transverse diffusion we need to know the behavior of the longitudinal one. The latter, calculated with a

similar procedure with the transverse diffusion, reads

$$\frac{D_{||}}{D_{||,0}} = (1 - \beta_{||}^{-1/2} L_e^3 \rho f_{||}(b_e/L_e))^2 \quad (3)$$

where $f_{||}(b_e/L_e) = C_{||}(b_e/L_e)[1 + (8/\pi - 1)C_{||}b_e/L_e]$ and $C_{||}$ and $\beta_{||}$ are constants.

Alternatively, the effect of head over head collisions during a longitudinal diffusive motion (jamming effect) can be treated in a critical hole model similar to that proposed by Cohen and Turnbul for liquids of small molecules.[7,20] In the "hole theory" the basic assumption is that the longitudinal motion of the test chain occurs only when a "hole" that is larger than a critical size exists in front of it. According to this approach the parallel diffusion coefficient reduces exponentially with concentration

$$\frac{D_{||}}{D_{||,0}} = \exp(-V^*_{ex}\rho) \quad (4)$$

with $V^*_{ex} = V(\lambda^* L_e, \lambda^* b_e, L, b)$, a function which expresses an excluded volume of the polymer chain and depends on the geometric parameters of the chain L, b and the dimensions $\lambda^* L_e$, $\lambda^* b_e$ of the critical hole. Thus, λ^* is the similarity ratio of the critical hole and the fuzzy cylinder and represents the strength of the effect of the head over head collisions on the slowing down of the parallel diffusion. Both approaches give a similar $D_{||}$ for relatively low concentrations (semidilute region); on the other hand, at high concentrations "hole theory" predicts an exponentially decreasing $D_{||}$ with concentration, whereas eq 3 predicts a cessation of parallel translational diffusion at a finite concentration, in qualitative agreement with the earlier predictions of Edwards and Evans[16] for the self-diffusion of highly entangled rodlike molecules. The average over all orientations self-diffusion coefficient which is the experimentally measured quantity in an isotropic solution is calculated then according to $D_s/D_{s,0} = (D_{||} + 2D_{\perp})/(D_{||,0} + 2D_{\perp,0})$ and eqs 2−4.

On the experimental side, there are some studies of the self-diffusion of wormlike polymers and rigid rod colloids that we summarize below. Tinland et al.[2] have used several molecular weights of wormlike xanthan (with $L = 10l$ to $200l$) and found a sigmoidal decrease of D_s with c (constant in the dilute, decreasing in the semidilute and leveling off in the concentrated region), except for the higher molecular weight where the decrease was monotonic. The decrease is more rapid for higher molecular weight and can be described only semiquantitatively for the three middle fractions by the "fuzzy cylinder" model predictions. An indication for a leveling off at higher concentrations was explained by the reptation mechanism that predicts a concentration independence of D_s. Latter Bu et al.[3] measured the self-diffusion of PBLG (with $L = 0.14l$ to $16l$) by FRAP and again found two or three regimes depending on the molecular weight. In contrast to Tinland et al., they found an indication of leveling off only for the two highest molecular weights. D_s starts to decrease well above the overlap number concentration $\rho^*(=1/L^3)$ but the data could not be represented by any analytical theory; they instead follow a power law, $c^{-1.13}L^{-1.8}$, dependence. In the above studies the cessation of motion suggested by Edward and Evans[16] and eq 3 was not observed. Concerning the level off of D_s at high concentrations for some of the measurements, Sato and Teramoto[7] have pointed out that it is in disagreement with the zero-shear viscosity dependence of c^3 to c^7 at high concentrations.[8] Only the very recent work by Ohshima et al.[10] on the mutual diffusion of PHIC in solutions presents a quantitative comparison of the indirectly deduced self-diffusion coefficient with the predictions of the fuzzy-cylinder model.

The "fuzzy cylinder" model also predicts the concentration dependence of the rotational diffusion and the zero-shear viscosity. These two properties are interrelated and furthermore depend on the behavior of the longitudinal diffusion. Doi[15] using the Kirkwood theory, calculated the stress tensor $\boldsymbol{\sigma}$ describing the stress induced in a homogeneous isotropic solution of stiff macromolecules by a macroscopic flow which can be decomposed into three terms, $\boldsymbol{\sigma} = \boldsymbol{\sigma}^{(E)} + \boldsymbol{\sigma}^{(V)} + \boldsymbol{\sigma}^{(S)}$, where $\boldsymbol{\sigma}^{(E)}$ is the elastic stress, $\boldsymbol{\sigma}^{(V)}$ the viscous stress arising from the polymer−solvent friction, and $\boldsymbol{\sigma}^{(s)}$ the contribution of the solvent. On the basis of the above the zero-shear viscosity calculated by the fuzzy cylinder model reads[6,7]

$$\eta_0 = \eta^{(S)} + \eta^{(V)} + \eta^{(E)} = \eta_s + (4/\gamma - 3\chi^2)\frac{\rho k_B T}{30 D_{R,0}} + \chi^2 \frac{\rho k_B T}{10 D_R} \quad (5)$$

where γ and χ are hydrodynamic factors which depend directly on the aspect ratio of the chain. In the same theoretical framework the rotational diffusion coefficient yields

$$\frac{D_R}{D_{R,0}} = \left(1 + \beta_R^{-1/2} L_e^4 \rho f_R(b_e/L_e)\sqrt{\frac{D_{R,0}}{6D_{||}}}\right)^{-2} \quad (6)$$

where β_R is a constant and $f_R(b_e/L_e) = (1 + C_R b_e/L_e)^3(1 - C_R b_e/5L_e)$ is a function of the fuzzy cylinder aspect ratio L_e/b_e. Similar to $C_{\perp}$, C_R assumes values ($0 < C_R < 1$) depending on the effectiveness of the mechanism of constraint release by segment fluctuation. The rotational diffusion in the dilute limit, $D_{R,0}$, has been calculated by Yoshizaki and Yamakawa[21] in the helical wormlike model. Using eq 5 together with eqs 6 and 4 (or eq 3) for the longitudinal diffusion coefficient, one ends up with the expression for the zero shear viscosity of solutions of wormlike chains.

The zero-shear viscosity has been measured for isotropic solutions of liquid crystalline polymers much more extensively than any other quantity, which relates to the dynamics of these systems due to the relative simplicity of the experiment. Measurements on aqueous xanthan solutions[7,8] have revealed a very strong concentration dependence of η_0 and a molecular weight dependence, which may exceed the scaling dependence $\eta_0 \sim M^{3.4}$ for high molecular weights of flexible chains. Similar behavior of the viscosity has been observed in other stiff-chain polymer solutions[7] such as several molecular weights of PHIC (with $L/l = 1.6-200$) studied[9] in a wide concentration range. In this study the predictions of the "fuzzy cylinder" model could fit the viscosity data only for $L/l < 20$ indicating the limitations of the model. The effect of polydispersity on the zero-shear viscosity of stiff polymers was investigated[8b] by using "quasi-ternary" solutions with several weight fractions of two fractionated xanthan samples to reveal a dependence on the weight-average molecular weight and not on the weight distribution itself.

Table 1. Molecular Characteristics of PPPS Samples

sample	M_w (g/mol)	L_w (nm)	L_w/L_n	$N = L_w/2l$	L_e (nm)	b_e (nm)	c^* (mg/cm^3)
S1	189 000	256	1.91	5.1	107	34	0.253
S3	113 000	153	2.09	3.55	80	24	0.368
S5	90 000	122	2.5	2.45	70	20	0.444
S7	40 000	54	1.82	1.1	40	9	1.043

Furthermore, an extension of the predictions of the fuzzy cylinder model for the zero-shear viscosity, the translational self-diffusion, and the rotational diffusion coefficients of semiflexible chains that incorporates intermolecular hydrodynamic interactions (HI) was presented by Sato et al.[22] and found to improve the representation of the zero-shear viscosity data.[10,22] The intermolecular HI were considered up to the linear term in polymer mass concentration, c, introducing an extra concentration dependence to all hydrodynamic quantities:

$$\hat{\eta}^{(V)} = (1-3\chi^2\gamma/4)[\eta]\eta_s c(1 + k_{HI}[\eta]c) \quad (7a)$$

$$\hat{D}_{R,0} = D_{R,0}/(1 + k_{HI}[\eta]c) \quad (7b)$$

$$\hat{D}_{\perp,0} = D_{\perp,0}/(1 + k_{HI}[\eta]c) \quad (7c)$$

$$\hat{D}_{||,0} = D_{||,0}/(1 + k_{HI}[\eta]c) \quad (7d)$$

Here $[\eta]$ is the intrinsic viscosity. The coefficient k_{HI} represents the strength of the intermolecular HI, which in principle may be different for each one of the above hydrodynamic quantities (eq 7). Nevertheless, in view of the lack of theoretical calculations or unambiguous experimental determination of these quantities for semistiff chains, we may use to a first approximation a single k_{HI}, which is treated as a fitted parameter.

III. Experimental Section

A. Materials. The molecular characteristics of the PPPS samples utilized are summarized in Table 1 where the overlap mass concentration is c^*. L_w is the weight-average contour length, M_w the weight-average molecular weight, $N = L_w/2l$ the ratio of the contour length to the Kuhn segment length ($2l$), and L_w/L_n the polydispersity. For the present wormlike chains the overlap number concentration ρ^* was approximated by $1/L_e^3$ as in the case of studies on other PPPSs.[1] The end-to-end distance, L_e, of a wormlike chain is given by $L_e = [2Ll - 2l^2(1 - \exp[-L/l])]^{1/2}$ and was calculated using the weight-average contour length L_w and a persistence length, $l = 25$ nm. In the framework of the wormlike model, the latter was determined by depolarized light scattering[24] and fits well the molecular weight dependence of the translational diffusion coefficient.[1] The ratio of the contour length to the Kuhn segment length, $N = L/2l$, ranges from 1.1 for the smaller molecular weight S7 to 5.1 for the higher S1.

The enhanced solubility of the present poly(*p*-phenylenes) in common organic solvents allows the study of the self-diffusion dynamics well into the concentrated region. The lack of isotropic to nematic transition up to high concentrations is characteristic of these hairy wormlike chains, an effect possibly due to the bulky side chains.[1] Solutions in toluene, used in both experiments, were prepared at low concentrations in the dilute or low semidilute regime, and higher concentrations were reached by slow evaporation of the solvent.

B. Pulsed Field Gradient (PFG) NMR. With PFG−NMR, the time self-correlation function of the positions of proton-bearing segments of polymer chains is measured.[25] When the mean square displacement during the observation time is larger than the radius of gyration, the self-diffusion of the center-of-mass of the chains is determined. Deuterated toluene was used as a solvent in the present study, to enable the selective observation of the macromolecular diffusion. The basic idea of PFG NMR is tagging of the nucleus with respect to its position in space by a spatially varying Larmor precession $\omega(z) = \gamma B(z)$; with γ being the gyromagnetic ratio of nucleus under study and $B(z) = B_0 + gz$ the total magnetic field composed of a constant field B_0 and a gradient gz.

The basic idea of the experiment is the stimulated echo experiment with a time sequence $\pi/2-\tau-\pi/2-t-\pi/2-\tau-$echo.[25] After the first and third $\pi/2$ radio frequency pulses, two field gradient pulses of magnitude g and duration δ are applied. The measured spin echo attenuation, A/A_0, (A_0 is the spin echo amplitude without applied field gradients) following the first and second $\pi/2$ radio frequency applied field gradient pulses is equivalent to the incoherent intermediate scattering function known from neutron scattering[26] $S_{inc}(q,t) = \int \exp(iqz)\, P(z,t)\, dz$. For free diffusion, the probability for a displacement of a polymer segment over the distance z within the diffusion time t, $P(z,t)$, is Gaussian, yielding $S_{inc}(q,t) = \exp(-q^2D_s t)$ with D_s being the self-diffusion coefficient and $q = \gamma\delta g$ the generalized scattering vector.

For polydisperse samples the measured quantity is an averaged, over the distribution of diffusion coefficients $W(D)$, incoherent structure factor, $S_{inc}(q,t) = \int W(D) \exp(-q^2Dt)\, dD$ The experimental $S_{inc}(q,t)$ functions were fitted using the log-normal distribution

$$W(\ln D) = \exp[-\ln^2(D/D_s)/2[\ln^2\sigma]]/(2\pi[\ln\sigma])^{1/2} \quad (8)$$

of the self-diffusion coefficient where the two fitting parameters are σ and the diffusion coefficient D_s, which corresponds to the maximum of $W(\ln D)$.[27] This distribution is based on the assumption of a log-normal molecular weight distribution and a power law relationship for D_s ($\propto M^{-\alpha}$). In this work the PFG−NMR experiments were carried out with a home-built NMR spectrometer operating at a ^{1}H-resonance frequency of 400 MHz at room temperature.[25] The time τ was kept fixed in our experiments at $\tau = 3$ ms. In one particular experiment δ and t were fixed and g was incremented. The maximum g value was 25 T m^{-1} and the maximum δ value was 1.85 ms. Diffusion times t were typically between 10 and 300 ms, while the sample was thermostated at a temperature of 25 °C.

C. Shear Rheology. The rheological properties of the wormlike polymers investigated were studied using shear rheometry in the dynamic and steady modes. A Rheometric Scientific constant strain rheometer (ARES-HR 100FRTN1 with a very sensitive dual range force rebalance transducer and a high-resolution actuator) was utilized. Measurements were carried out in the cone-and-plate (25 mm diameter, 0.04 rad cone angle) or Couette (height 10 mm, gap 1 mm, used for the very dilute samples) geometries at room temperature (25 °C, with temperature control achieved via a recirculating fluids bath) and in an atmosphere saturated in solvent (toluene) to eliminate evaporation during measurements. The linear viscoelastic moduli (storage, G' and loss G'') of the solutions of S1, S5, and S7 at various concentrations were measured using small-amplitude oscillatory shear experiments. Dynamic strain sweeps (at constant frequencies of 0.1, 1, and 10 rad/s, with varying strain amplitude from 1 to 100%) were conducted in order to identify the region of linear viscoelasticity. Dynamic frequency sweeps (at constant linear strain, and frequency ranging from 500 to 0.05 rad/s) were performed to map the linear viscoelastic spectra of G' and G''. Steady shear rate sweep tests were performed from 0.01 to 500 s^{-1} in order to obtain their rheograms and thus determine the zero shear viscosity, η_0. For the highest concentrations, and in particular for $c \geq 7.5\%$ (by mass) for polymer S1, where the Newtonian plateau could not be reached, η_0 was determined from fitting

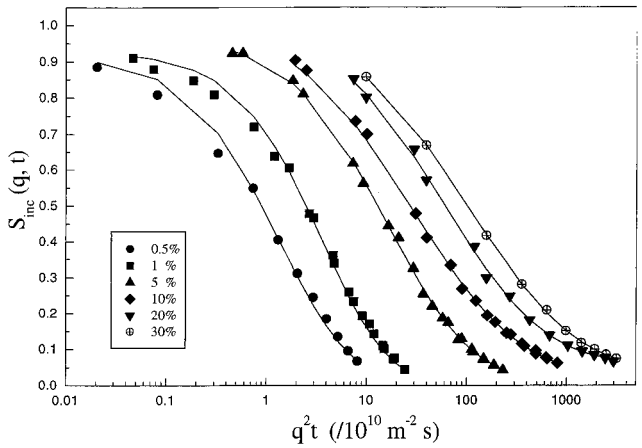

Figure 1. Experimental incoherent structure functions of S7 toluene solutions at 25 °C, with weight percent concentrations as follows: 0.5% (●), 1% (■), 5% (▲), 10% (◆), 20% (▼), and 30% (⊕). Lines are best fits according to $S_{inc}(q,t) = \int W(D) \exp(-q^2 Dt)\, dD$ with $W(\ln D)$ given by eq 8.

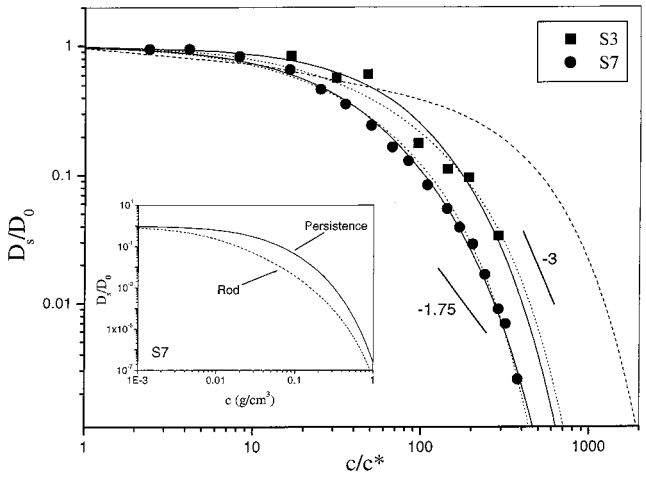

Figure 2. Concentration dependence of the normalized self-diffusion coefficient, D_s/D_0, vs the reduced concentration c/c^* for the two molecular weights: (■) S3 and (●) S7. The solid lines indicate fits according to the eq 10 with intermolecular hydrodynamic interactions, while the dotted lines represent eq 10 with zero intermolecular HI. The two straight solid lines represent the scaling predictions for flexible chains in good and Θ solvents. The dashed line is the theoretical prediction for a rodlike polymer with the same length with S7. Inset: predictions for a rodlike chain and fuzzy cylinder chain with the same parameters with sample S7 against the weight concentration.

of the shear viscosity data $\eta(\dot\gamma)$ using the Carreau empirical model:[28]

$$\frac{\eta - \eta_\infty}{\eta_0 - \eta_\infty} = \frac{1}{[1 + \tau_l^2 \dot\gamma^2]^{(1-n)/2}} \tag{9}$$

where η_∞ is the infinite-shear viscosity, τ_l the longest relaxation time and n a power-law coefficient; all three were treated as adjustable parameters. Alternatively, the dynamic frequency sweep data (in the region where the terminal scalings $G' \sim \omega^2$ and $G'' \sim \omega$ were not reached) were represented by means of a relaxation time spectrum according to the analysis of Baumgaertel et al.,[29] and η_0 was subsequently obtained. In a few concentrations, both methods were used: the results were in good agreement, and in the discussion below, average values of η_0 were used.

IV. Results and Discussion

A. Self-Diffusion. The incoherent structure factor, $S_{inc}(q,t)$, of wormlike PPPS in toluene was measured over a wide concentration range from the marginally dilute regime ($c \sim c^*$) up to highly concentrated region ($c \approx 1000c^*$) for two different molecular weights S3 and S7 (Table 1). The experimental $S_{inc}(q,t)$ measured by PFG−NMR is shown in a linear−logarithmic plot in Figure 1 against q^2t, for solutions of S7 at several concentrations in *d*-toluene at 25 °C. There is an obvious slowing down of the incoherent structure factor as concentration is increased. The fit of $S_{inc}(q,t)$ was performed utilizing the log-normal distribution of D (eq 8) with D_s and σ as fitting parameters.[27]

Figure 2 depicts the plot of D_s normalized to its infinite dilution value D_0 against the normalized to c^* concentration, c/c^*, for the S3 and S7 solutions. We observe the sharp decrease of the self-diffusion a result of both the intermolecular steric interactions (or entanglement effects), and the intermolecular HI as described by eqs 2−4 and eq 7, parts c and d. The data do not superimpose on one curve in this normalized D_s/D_0 vs c/c^* plot as one would expect for semidilute solutions of linear flexible macromolecules according to scaling predictions,[15] which are denoted by the two slopes in Figure 2 (for good solvent conditions $D_s \propto c^{-1.75}$; for Θ solvent conditions $D_s \propto c^{-3}$). However, plots of the experimental log D_s against log c for various flexible polymers in solution usually reveal curves of progressively increasing curvature rather than the straight lines predicted by scaling theory. On the other hand such a smooth increase of curvature results at high concentrations to steeper than the c^{-3} decrease of D_s which is described by the fuzzy cylinder model (eqs 2−4) and moreover has been observed experimentally.[7,10]

The predictions of the fuzzy cylinder model for the transport properties namely the self-diffusion, the rotational diffusion and the related to the latter zero-shear viscosity depend on the behavior of the longitudinal diffusion as can be seen in eqs 2−7. The mean field Green function approach (eq 3) predicts a cessation of parallel diffusion at $\rho \sim \beta^{1/2}/f_{||}L_e$, similarly to the Edwards−Evans prediction for rigid rods,[16a] which nevertheless has not been seen experimentally. On the other hand "hole theory" predicts an exponential decrease of the parallel diffusion coefficient with concentration (eq 4) that is comparable with the decrease of the self-diffusion predicted by Edwards and Vilgis[16b] for a system of cooperatively moving rigid rods. The former combined with the proposed corrections for the intermolecular HI (eq 7) leads to a self-diffusion coefficient

$$D_s/D_0 = [\exp(-Ax) + 2C(1 + Bx \exp(Ax/2))^{-2}]/[(1 + 2C)(1 + Kx)] \tag{10}$$

where $x = c/c^*$ is the normalized concentration, $A = V_{ex}^*/L_e^3$ is a normalized excluded volume parameter, $B = f_\perp(2D_{\perp,0}/\beta_\perp D_{||,0})^{1/2}$ is a constant, and $K = k_{HI}[\eta]M/L_e^3 N_A$ represents the strength of the intermolecular HI. Prior to the representation of $D_s(c)$ by eq 10, we discuss the values of fixed parameters, L_e, b_e, C, $C_\perp$, $f_\perp$. While theoretical expressions of L_e exist in the framework of the wormlike model, there is no explicit calculation of b_e. Thus, for the latter we used Hoshikawa et al.'s result[30] which is based on a model by Tagami[31] and is considered a good approximation for a wormlike chain.[7] Furthermore, the ratio of the transverse to the longitudinal diffusion coefficients in the limit of infinite dilution, C, has not been formulated for a wormlike

Table 2. Hydrodynamic Parameters for PPPS Samples

sample	$C = D_{\perp,0}/D_{\|\|,0}$	D_0 ($/10^{-7}$cm^2/s)	$f_\perp$	f_R	γ	χ
S1	0.806	1.98	1.282	1.664	0.077	0.847
S3	0.798	2.81	1.156	1.35	0.072	0.866
S5	0.795	3.29	1.125	1.276	0.07	0.871
S7	0.767	5.85	1.058	1.125	0.051	0.924

chain and thus can only be approximately estimated[6,7] by that of an ellipsoid of revolution with the same aspect ratio $p_e = L_e/b_e$. The function $f_\perp$ (eq 2) depends on the inverse aspect ratio, $1/p_e$, and the constant $C_\perp$, which represents the effectiveness of the hindrance release through the fluctuation of segments mechanism. The latter has been expressed[7] empirically by a formula with two adjustable parameters N^* and Δ to describe the N dependence of zero-shear viscosity data of several solutions of stiff macromolecules like aqueous xanthan and schizophyllan[6] and PHIC.[9,10] Here we use the same values that have been used[7] for PHIC ($N^* = \Delta = 4$) which has a persistence length (21 nm)[7] similar to that of the PPPS (25 nm).[1]

Thus, we end up with three floating parameters, A, B, and K, (eq 10) which relate to V^*_{ex}, $\beta_\perp$, and k_{HI}, respectively. As mentioned in section II, the excluded volume parameter V^*_{ex} involves a similarity parameter λ^* which relates the true dimensions of the chain to the dimensions of the hole which is introduced to describe the slowing down of the longitudinal diffusion. The parameters involved in both D_s and η_0 are λ^* and k_{HI}, while $\beta_\perp$ is involved only in the calculation of D_s and β_R in that of η_0. Note that although there are calculations of β_R and $\beta_\perp$ for long thin rods, there is none for semiflexible chains and thus we chose to treat them as fitting parameters. To quantitatively test the predictions of the fuzzy cylinder model, we seek for common set of physically meaningful parameters that can simultaneously represent D_s and η_0 for all molecular weights. Table 2 lists the fixed values of the hydrodynamic parameters used in the fitting procedure of both the self-diffusion and the viscosity data.

Figure 2 shows the best fits according to eq 10 for the concentration dependence of D_s for the two PPPS samples (S3 and S7). The data were fit both with and without intermolecular HI introduced in eq 10 by the correction term $(1 + Kx)$ in order to assess the influence of such effects. The solid lines represents eq 10 with parameters $\lambda^* = 0.084$ for both molecular weights and $k_{HI} = 0.021$, $\beta_\perp = 26316$ for S3 and $k_{HI} = 0.095$, $\beta_\perp = 5937$ for S7. Both fits are quite satisfactory, implying that the fuzzy cylinder model together with the "hole theory" can capture the general features of self-diffusion dynamics of wormlike polymer solutions. We believe that flexibility effects are responsible for the much larger values of $\beta_\perp$ compared to the rigid rod estimation ($\beta_\perp = 561$) for both samples. In general, $\beta_\perp$ and β_R are quantities that represent the maximum crowding of chains in a volume of L_e^3 that the system can tolerate before losing some of its translational and rotational freedom, respectively. Thus, we may reasonably expect that $\beta_\perp$ and β_R are larger in solutions of semiflexible chains than in solutions of rigid rods. In this sense the significantly higher value of $\beta_\perp$ (=26 316) representing the D_s data of S3 may relate to chain conformation resembling a wormlike coil ($N = 3.55$) whereas the lower $\beta_\perp$ value for S7 (=5937) refers to a less bended chain ($N = 1.1$). The values of λ^* for both samples are similar to the one used to quantitatively describe the self-diffusion and the zero-shear viscosity data of aqueous solutions of xanthan[6,7] ($\lambda^* = 0.11$). In other experimental works, smaller values of λ^* were found[7]—$\lambda^* = 0.05$ for PPTA solutions and $\lambda^* = 0.03$ for PBLG solutions—while a representation of simulation results of rigid rods[32] with the "hole theory" yielded the smallest values[7] of $\lambda^* = 0.025$. We must also note that the same analysis was unsuccessfully applied to semiflexible ladder-type polymer chains[33] in solution where the self-diffusion data could be fitted only with unrealistically small values for V_{ex} resulting in negative values for λ^*. The failure of the fuzzy cylinder model was then attributed to the high flexibility of those chains (their persistence length was found to be three times smaller than that of the present system).

In all studies mentioned above, the effects of intermolecular HI were ignored. More recently, however, viscosity data[10,22] of PHIC solutions together with self-diffusion data[10] deduced from light scattering measurements of the cooperative diffusion coefficient were successfully compared with the improved version[22] of the fuzzy cylinder model where intermolecular HI were incorporated. The authors claimed that this expansion of the theory provides a better fitting of the viscosity data.[10,22] One apparent effect of the inclusion of intermolecular HI's is the increase of λ^* from 0.03 in the absence[9] of the HI term in eq 7a, to 0.06 with[22] HI. We should mention that in this type of analysis the rodlike values of both $\beta_\perp$(=561) and β_R (=1350) were used. In our work both the self-diffusion and the viscosity data (see below) cannot be fitted consistently using these rodlike values, implying the need to use higher $\beta_\perp$ and β_R values, which in our opinion is characteristic of semiflexible chains.

In an attempt to clarify the role of the intermolecular hydrodynamic interactions in the description of our experimental data, we fit D_s (as well as the η_0 which is discussed latter), keeping $K = 0$. The dotted lines in Figure 2 represent eq 10 without HI and correspond to $\beta_\perp = 21\,323$ and $\lambda^* = 0.09$ for the large molecular weight S3 and $\beta_\perp = 2354$ and $\lambda^* = 0.12$ for the smaller molecular weight sample S7. The basic conclusion from these fittings is that the fuzzy cylinder model without HI cannot describe the experimental c dependence of the self-diffusion at different molecular weights with a common set of parameters λ^* and $\beta_\perp$. The dashed line of Figure 2 shows the theoretical prediction of D_s for a rodlike polymer with a contour length equal to that of S7, $\beta_\perp = 561$ (the rodlike estimation), $\lambda^* = 0.084$, and no HI. Although plotted against c/c^*, it appears to decrease much less than D_s of a fuzzy cylinder; this is due to the much smaller value of c^* ($=1/L_e^3$), for a rod with the same contour length (since $L_e < L$), rather than to a weaker intrinsic slowing down as may be seen in the inset of Figure 2 where D_s of a rigid chain and a stiff chain of the same contour length is plotted vs c.

B. Friction Coefficients. A comparison of the self-diffusion coefficient deduced from the PFG–NMR incoherent structure factor with the cooperative diffusion coefficient measured by light scattering in our previous work[1] is shown in Figure 3. Whereas the self-diffusion (D_s) of the polymer chain becomes slower as the concentration increases due to strong intermolecular hindrance, the cooperative diffusion (D_c) speeds up with increasing concentration reflecting the dominance of the osmotic pressure contribution $(\partial\pi/\partial c)_{T,P}$ over friction, f_c, comprised in the cooperative diffusion coefficient $D_c =$

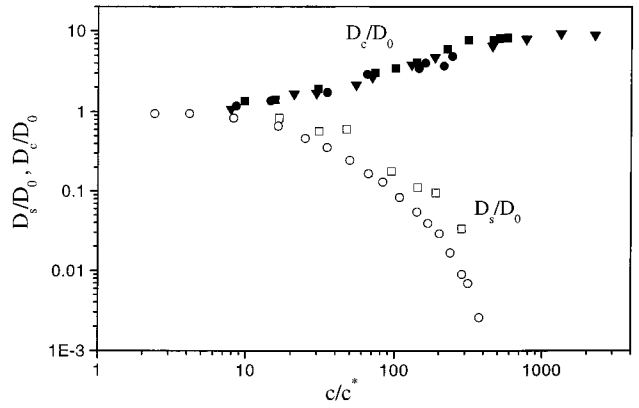

Figure 3. Concentration dependence of the normalized self-diffusion coefficient, D_s/D_0, (open symbols) and the normalized cooperative diffusion coefficient D_c/D_0, (solid symbols) vs the reduced concentration c/c^* for all molecular weights: (▼) S1, (■,□) S3, (●, ○) S7, and (◆) S9. The cooperative diffusion data measured by dynamic by light scattering are taken from ref 2.

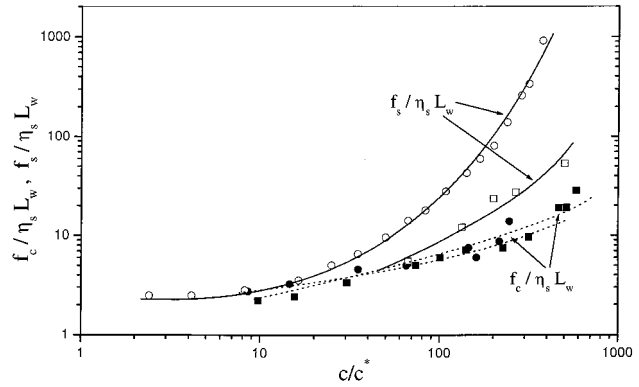

Figure 4. Concentration dependence of the cooperative friction, $f_c/\eta_s L_w$, (■) S3 and (●) S7, and the self-diffusion friction, $f_s/\eta_s L_w$, (□) S3 and (○) S7, normalized by the solvent viscosity and the weight-average contour length.

$(M/N_A)(1 - \phi)(\partial\pi/\partial c)_{T,P}/f_c$, and the consequent suppression of concentration fluctuations. Furthermore, a comparison of the self-friction coefficient, $f_s = k_B T/D_s$, with the cooperative one, f_c, is shown in Figure 4 for the two fractions S3 and S7. The concentration dependence of the unitless ratio, $f_s/\eta_s L_w$, of the friction coefficients to the solvent viscosity and weight-average contour length of the polymer chain clearly reveals the different character of the two frictions. The self-friction increases faster than the cooperative friction for the present PPPS samples as well as for ladder-type semiflexible polymers[33] while similar differences between f_c and f_s have been found in other stiff polymers such as PBLG solutions.[4] The cooperative friction coefficient, related to the response of the system to concentration fluctuations, involves both self- and cross-correlation terms of the velocity of the solute particles; the latter distinguish it from the self-friction coefficient involving only velocity self-correlation contributions.[11] This difference renders the use of techniques that measure cooperative effects, such as light scattering rather unsafe for the determination of the self-diffusion coefficient even when static and dynamic measurements are utilized to determine the osmotic compressibility and the cooperative diffusion coefficient.

Another important finding is that the self-friction per unit length (Figure 4) is higher for the short polymer chain (S7) than for the long one (S3) whereas the cooperative friction per unit length assumes similar values for the two samples supporting the suggestion that the two coefficients are of different nature. This dependence of the friction coefficient may be attributed to flexibility and is in qualitative agreement with the behavior of the characteristic relaxation time measured by depolarized light scattering[1] which relate with the rotational diffusion of Kuhn segments of the polymer chain and exhibit a much stronger decrease with c for the short than for the long chain. It is also reflected to the smaller values of $\beta_\perp$ for the short S7 sample compared to the longer S3 as was discussed above. The same molecular weight dependence of f_s is found in PBLG solutions[4] where the self-diffusion was measured by FRAP.

We believe that both the difference of the self-and cooperative friction and the molecular weight dependence of the former are important findings coming from independent measurements and their understanding is one of the open questions for future experimental and theoretical study.

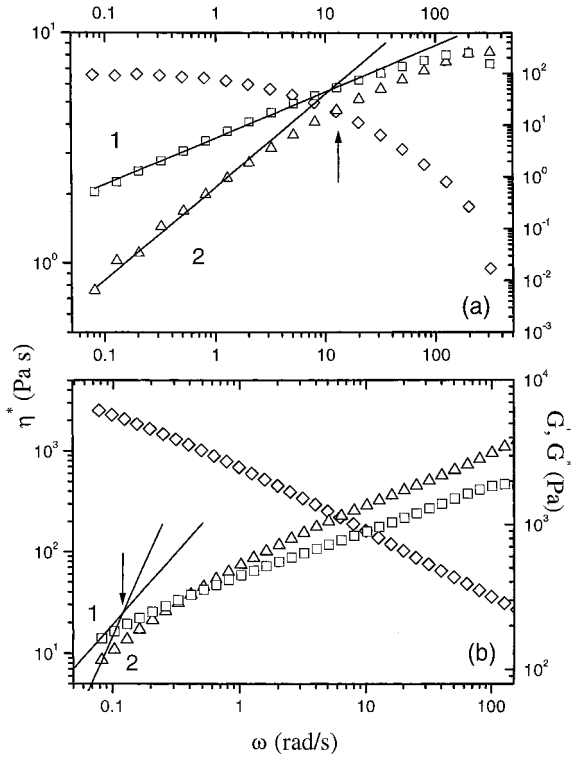

Figure 5. Frequency dependence of the dynamic shear moduli (storage, G', △; loss, G'', □) for two S1 solutions in toluene (8% and 18%) at 25 °C. The $G' - G''$ crossover identifies the longest relaxation time (vertical arrow). The complex dynamic shear viscosity, *y*ielding the solution's zero-shear viscosity, η_0, is also shown in the plot (◊). Slopes indicate the scaling of the terminal regime.

C. Zero-Shear Viscosity. The self-diffusion measurements by PFG−NMR are complemented with information on the dynamic shear moduli for three PPPS samples at different concentrations. Figure 5 shows the storage, G', and loss moduli, G'', and the complex viscosity, η^*, as a function of the frequency, ω, for solutions of S1 at two different concentrations, 8% and 18%, by weight in toluene at 25 °C. It is evident from the linear viscoelastic data that both solutions form a transient network characterized by the solidlike response ($G' > G''$) at high frequencies, which relaxes at low frequencies. The onset of terminal relaxation is

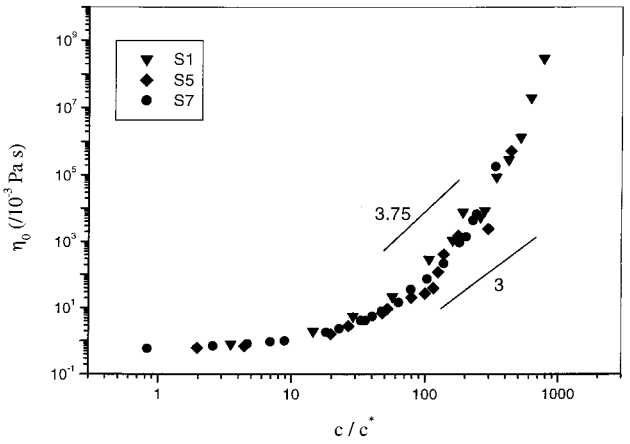

Figure 6. Concentration dependence of the zero-shear viscosity, η_0, for the three samples (▼) S1, (◆) S5, and (●) S7. The slope of 3 is the c dependence according to Doi−Edwards model for rigid rods, whereas the slope of 3.75 represents the experimental evidence for flexible chains.

marked by the crossover frequency to liquidlike behavior ($G'' > G'$). For the 8% S1 solution the standard terminal flow scaling behavior[34] ($G' \sim \omega^2$ and $G'' \sim \omega$) has been reached, which allows the straightforward estimation of the longest chain relaxation time τ_l, by extrapolation of the terminal G' and G'' lines. They intersect at a frequency which is slightly lower than the crossover frequency, apparently due to the polydispersity of the samples (see also Table 1). On the basis of these considerations, in the absence of aggregation problems, we identify the crossover frequency as the inverse of the characteristic chain relaxation time, τ_l, which is indicated by vertical arrows in Figure 5. On the other hand, for the more concentrated S1 solutions (c > 15%) the terminal flow has not been reached within the experimentally accessible frequency window (Figure 5b), whereas the principle of time−temperature superposition is not applicable here due to solvent evaporation at high temperatures and aggregation at low temperatures; consequently, the experimental error in the determination of the longest relaxation time, τ_l, is higher for these high concentration measurements.

The concentration dependence of the zero-shear viscosity is shown in Figure 6 for all three samples (S1, S5, S7). The viscosity−concentration superposition for different molecular weights is predicted by scaling theory and experimentally found for flexible chains[15] ($\eta_0 \sim c^{3.75}$). For the wormlike polymers under study besides some scatter of η data at high concentrations, the data for different molecular weights superimpose when plotted against c/c^* in contrast to the self-diffusion data. Note that the overlap concentration, c^*, was determined using the weight-average contour length, L_w (needed to calculate L_e) whereas when the number-average value is used the superposition of the viscosity data is not as good. The most important finding though, is that the measured solution viscosities exhibit a much stronger than the c^3 dependence expected for rodlike polymers if eq 5 and the Doi−Edwards prediction for the rotational diffusion ($D_R \sim c^{-2}$) are used. This finding is in qualitative agreement with the sharp slowing down of the decay rate in depolarized dynamic light scattering measurements found for these wormlike chains[1] as well as with the concentration dependence of η_0 for other solutions of wormlike polymers such as aqueous solutions of xanthan[7,8] and solutions of PHIC.[9,10]

Table 3. Experimental Intrinsic Viscosity, [η], from the Present Work and the Work of Vanhee et al.[35] Together with the Theoretical Value Calculated from the Wormlike Rotational Diffusion Coefficient $D_{R,0}$

sample	$[\eta]^{34}_{exp,in\ THF}$ (cm^3/g)	$[\eta]_{exp,in\ toluene}$ (cm^3/g)	$D_{R,0}$ (s^{-1})	$[\eta]_{theory}$ (cm^3/g)
S1	331	520	12 573	3222
S3	180		30 161	2403
S5	127	130	45 234	2069
S7	67	90	223 293	1295

For a quantitative comparison of the viscosity data with theoretical predictions of the fuzzy cylinder model, we combine eq 5 for η_0 with eq 6 for $D_R/D_{R,0}$ and take into account the intermolecular HI of eq 7. The introduction of $D_R/D_{R,0}$ entails the use of $D_{||}/D_{||,0}$ which, taking into account the ability of "hole theory" to fit the self-diffusion data, is taken from eq 4. Thus, the zero-shear viscosity, which in general is related with the rotational diffusion coefficient, can be expressed in terms of the parallel self-diffusion coefficient. Consequently, the self-diffusion, the zero-shear viscosity and the rotational diffusion should in principle be fitted in the framework of the fuzzy cylinder model using the same parameters. Combining eq 5 and eq 7, the normalized viscosity reads

$$\frac{(\eta_0-\eta_s)}{c[\eta]\eta_s} = (1 + Kx)\left(1 + \frac{3}{4}\gamma\chi^2[(1 + Ex\exp(Ax/2))^2 - 1]\right) \quad (11)$$

with $E = \beta_R^{-1/2} L_e f_R (D_{R,0}(1 + 2C)/18D_0)^{1/2}$ In eq 11, γ and χ are hydrodynamic factors which have not been calculated for wormlike chains and, therefore, as in the case of C, are approximated by the values calculated for spheroid-cylinders[22] with the same aspect ratio (Table 2). In the process of representing the viscosity data by eq 11, since A results from the fit of D_s, there are only two fitting parameters, E and K, which relate with β_R and k_{HI}, respectively. The rest of the parameters involved in E and eq 11, namely L_e, C, γ, χ, $D_{R,0}$ and D_0 are calculated from the molecular parameters of the chain L_w, b, and M_w. Combining eq 5 and 6, the rotational diffusion coefficient can be related to the intrinsic viscosity through $\rho k_B T/D_{R,0} = (15/2)c[\eta]\eta_s\gamma$. However, this relationship along with the theoretical values of $D_{R,0}$ from the wormlike model calculations of Yoshizaki and Yamakawa[21] predicts a value of [η] that disagrees with the experimental values from the present work as well as measurements of the same polymers in THF.[35] As can be seen in Table 3 the discrepancy is rather high (the theoretical values of [η] are about 10 times larger than the experimental ones); consequently the use of the theoretical $D_{R,0}$ to estimate parameter E found in eq 11 by fitting the viscosity data becomes questionable for these wormlike chains. Instead, we choose to use the experimental [η] in the calculation of the left-hand side of eq 11 as well as in the evaluation of β_R from the fitting parameter E utilizing the relation between $D_{R,0}$ and [η].

In eq 6, the function $f_R(b_e/L_e) = (1 + C_R b_e/L_e)^3(1 - C_R b_e/5L_e)$ involves the constant C_R, which represents the effectiveness of the chain release mechanism through segment fluctuations in the rotational motion and similarly to $C_\perp$ takes values between zero (highly effective release) and one (ineffective release); here C_R is taken to be equal to $C_\perp$. Consequently E involves only one unknown, the constant β_R, which is treated as a fitting parameter. The value of β_R has been estimated

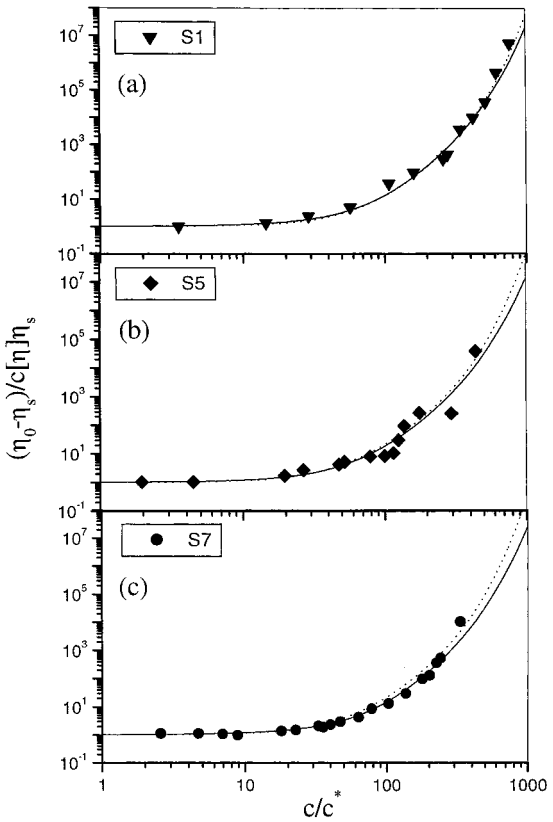

Figure 7. Concentration dependence of $(\eta_0 - \eta_s)/c[\eta]\eta_s$, for the three samples (a) S1 (▼), (b) S5 (◆), and (c) S7 (●), together with the fit according to eq 11. The solid line is the best fit taking into account the intermolecular HI while the dotted lines represent eq 11 in the absence intermolecular HI.

Table 4. Fitting Parameters from the Concentration Dependence of D_s and η_0 Using the Fuzzy Cylinder Model and "Hole Theory" along with the Correction for the Intermolecular HI

sample	λ^*	$\beta_\perp$	β_R	$k_{HI,\eta}$	$k_{HI,\,Ds}$
S1	0.084		3720	0.076	
S3	0.084	26 316			0.021
S5	0.084		3208	0.173	
S7	0.084	5937	2698	0.138	0.095

Table 5. Fitting Parameters from the Concentration Dependence of D_s and η_0 Using the Fuzzy Cylinder Model and "Hole Theory" without the Correction for the Intermolecular HI

sample	λ^*	$\beta_\perp$	β_R
S1	0.106		2250
S3	0.09	21 323	
S5	0.11		1784
S7	0.12	2354	947

theoretically by Teraoka et al.[36] for infinitely thin rods ($\beta_R = 1350$) using the notion of the cage model, and thus in accordance with the discussion for $\beta_\perp$, the result of the fit for these wormlike polymers may be expected to be larger than the thin rod value.

The concentration dependence of the reduced viscosity $(\eta_0 - \eta_s)/c[\eta]\eta_s$ for the three samples S1, S5, and S7 is shown in Figure 7. The solid and dotted lines correspond to representations of eq 11 with and without intermolecular HI, respectively. The simple version of eq 11 without intermolecular HI can represent the data successfully for all molecular weights with the parameters listed in Table 5. The values of λ^* used for S1 ($\lambda^* = 0.106$) and S5 ($\lambda^* = 0.11$) are similar to those used for the fit of D_s; note that for S7 we have used exactly the same value used to fit D_s ($\lambda^* = 0.12$). At the same time, β_R as estimated from the parameter E assumes the value of 2250 for S1, 1784 for S5, and 947 for S7. In accordance with the values of $\beta_\perp$, these values suggest that increasing contour length results in higher relative translational and rotational mobility at the same c/c^*. Thus, the representation of the self-diffusion and zero-shear viscosity data by the fuzzy cylinder model in the absence of intermolecular HI provides a value of λ^* around 0.1 and values $\beta_\perp$ and β_R which increase with increasing molecular weight and exceed the rodlike estimation. The latter is in agreement with the increasing intrinsic friction ($f_s/\eta_s L_w$) with decreasing contour length (Figure 4).

The apparent indictment of a nonuniform λ^* values in the simplified version of the fuzzy cylinder model may be rectified with the incorporation of intermolecular HIs which are introduced phenomenologically through the term $(1 + k_{HI}[\eta]c)$ in eqs 10 and 11, increasing the number of fitting parameters by one. The values of all fitting parameters from the representation of D_s (Figure 2) and η_0 (Figure 7) are listed in Table 4. For all molecular weights both D_s and η_0 are fitted with a single value of λ^* (=0.084) while $\beta_\perp$ and β_R increase with molecular weight, in qualitative agreement with their behavior in the absence of HI. The value of β_R is found to be larger than the thin rod prediction ($\beta_R = 1350$) which is in agreement with the respective $\beta_\perp$ for the perpendicular to the long axes self-diffusion. Nevertheless, a possible drawback of this procedure is that the self-diffusion and viscosity data cannot be fitted with the same value of k_{HI}; as can be seen in Table 4 the values of k_{HI} used to represent η_0 are larger ($k_{HI} = 0.076$ for S1, 0.173 for S5, and 0.138 for S7) than those used to fit D_s ($k_{HI} = 0.021$ for S3 and 0.095 for S7). On the other hand, this may suggest that the simplification we did in assuming the intermolecular HI parameters involved in all hydrodynamic quantities, $\hat{D}_{R,0}$, $\hat{D}_{\parallel,0}$, $\hat{D}_{\perp,0}$, and $\hat{\eta}^{(V)}$ in eq 7, the same is probably wrong. In principle, k_{HI} should be different for each one of these quantities, reflecting the influence of intermolecular hydrodynamic interactions on the rotational and longitudinal or transverse translational motion. In this context, our data imply that intermolecular HI affects less the translational than the rotational motion and hence the zero-shear viscosity.

Although the description of the concentration dependence of both the self-diffusion and the viscosity data by the fuzzy cylinder model and the hole theory is fairly successful, the resulting values for $\beta_\perp$ and β_R as well as the difference in the values of k_{HI} needed to fit D_s and η_0 suggest the necessary future refinements of the theory. Evidently a theoretical calculation of $\beta_\perp$ and β_R for wormlike chains and a further study of the effect of intermolecular HI in these different dynamic quantities, although probably is a formidable task, we believe is necessary, together with further critical comparisons with experimental data of different semiflexible polymers, for the final justification of the theory.

D. Longest Relaxation−Rotational Diffusion. It is interesting to compare the concentration dependence of the self-diffusion measured by PFG−NMR, the relaxation rates deduced from depolarized dynamic light scattering and dynamic rheology, and the zero-shear viscosity of stiff polymer solutions. In the framework of the fuzzy cylinder model a reduced viscosity, η_c, which

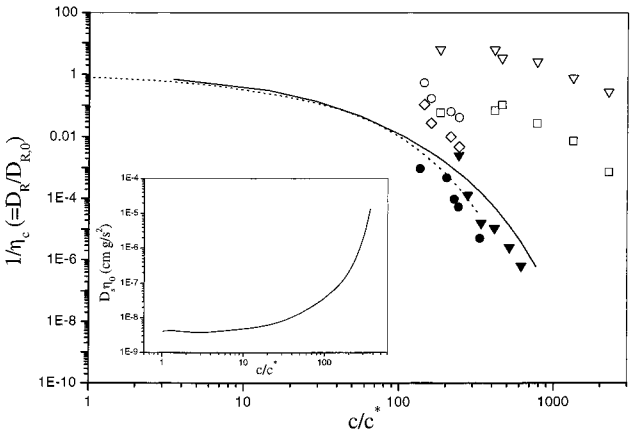

Figure 8. Concentration dependence of the reciprocal reduced viscosity, $1/\eta_c$ (S1, solid line, and S7, dotted line), together with the reduced rate of the longest chain relaxation time, $\Gamma_l/D_{R,0}$, extracted from rheological measurements (S1, ▼; S7, ●). The rates of the two relaxation processes measured by dynamic depolarized light scattering, $D_{VH}/D_{R,0}$, are also shown (S1, fast mode (▽) and slow mode (□); S7, fast mode (○) and slow mode (◇)). Inset: Concentration dependence of the product of the self-diffusion coefficient with the zero-shear viscosity, $D_s\eta_0$, for S7 (solid line).

is equal to the reciprocal of the reduced rotational diffusion coefficient $D_R/D_{R,0}$ may follow from eqs 5−7

$$\eta_c \equiv \frac{4}{3\gamma\chi^2}\left[\frac{(\eta_0-\eta_s)/\eta_s}{c[\eta]}\frac{1}{\hat{h}(c)} - 1\right] + 1 = D_{R,0}/D_R \qquad (12)$$

with $\hat{h}(c) = 1 + k_{HI}[\eta]c$ being the intermolecular HI contribution to the viscosity. Thus, we may compare $1/\eta_c$ from viscosity data with the relaxation times measured by depolarized light scattering in ref 1, as well as with the longest relaxation time determined in this work by dynamic shear rheology. We should recall that in the depolarized light scattering two relaxation processes of orientation fluctuations were detected and attributed to the collective rotational motion of the Kuhn segments of the chains (fast mode) and to the cooperative motion of orientationally correlated pairs of Kuhn segments (slow mode).[1] In Figure 8, we show $1/\eta_c$ and $D_{VH}/D_{R,0}$ for both depolarized scattering modes (open symbols) along with the ratio, $\Gamma_l/D_{R,0}$, of the decay rate of the chain relaxation rate, Γ_l (=$1/\tau_l$), to $D_{R,0}$ (solid symbols) for the two extreme molecular weights S1 and S7. Γ_l was estimated from the crossover of $G' - G''$, signifying the onset of the terminal regime as discussed above. Both relaxation processes from the depolarized light scattering measurements are much faster and display a weaker c dependence than the corresponding from the viscosity data and the longest relaxation time, indicating the different nature of these modes as discussed in ref 1. On the other hand, the decay rate of the chain relaxation time is slower than the $D_R/D_{R,0}$ obtained from the zero-shear viscosity data for both molecular weights although they exhibit the same concentration dependence. In the inset of Figure 8 the concentration dependence of the product of the self-diffusion coefficient with the zero-shear viscosity, $D_s\eta_0$, is shown for S7. It is apparent that the rise of the viscosity is much more rapid than the decrease of self-diffusion at $c > 10c^*$, whereas the longest relaxation time, which is directly related with the overall rotational motion of the chain, follows $1/\eta_c$ (=$D_{R,0}/D_R$) as anticipated from eq 2−7). This behavior reflects the fact that the rotational diffusion, and consequently the viscosity ($\propto\rho/D_R$), slows down faster than the self-diffusion. The discrepancy between the relaxation rates measured by depolarized light scattering[1] and the longest relaxation time determined by rheometry is expected since the latter relates to the overall rotation of the wormlike chain whereas the former as has been discussed previously relates with rotation of a smaller part of the chain namely the Kuhn segment. That is why this discrepancy is larger for the longer chain, S1 ($N = 5.1$).

V. Concluding Remarks

The present study has presented experimental data of the self-diffusion coefficient the zero-shear viscosity and the longest relaxation time of wormlike polymers in nondilute solutions over a broad concentration range and compared these results with predictions of the fuzzy cylinder model with and without intermolecular HI. The direct measurement of the self-diffusion by PFG−NMR and the comparison with data of the cooperative diffusion measured by dynamic light scattering verifiy the different nature of the self-and cooperative friction coefficients.

The comparison of the predictions of the fuzzy cylinder model with experimental findings was fairly successful validating the use of this model to describe the dynamic behavior of wormlike polymers in nondilute solutions. The possible drawback of the model in the absence of intermolecular HI, namely the inability to provide a fit for all molecular weights with a single λ^* is surpassed with the extended version of the model which incorporates intermolecular HI. In this way we found $\lambda^* = 0.084$, a value similar to that for other semiflexible polymers, while the $\beta_\perp$ and β_R values increase with chain length and are larger than the rodlike estimation. Nevertheless, the fact that several of the parameters involved in the theoretical expressions have not been calculated for wormlike chains together with the finding that the fitting parameters $\beta_\perp$ and β_R are systematically larger than the estimation for rodlike particles suggests that further theoretical work is needed, especially in the calculation of these parameters for wormlike chains. The increasing values of $\beta_\perp$ and β_R with increasing contour length together with the lower intrinsic self-friction ($f_s/\eta_s L_w$) for longer chains support the notion of a stronger effect of entanglements in the dynamics of shorter chains which although they exhibit a more rodlike shape they still have the same persistence length. Concerning the intermolecular HI effects it is found that the fitting of D_s and η_0 data requires the use of different values of k_{HI}, implying the different effect of intermolecular HI in the translational and rotational motion.

Finally, the concentration dependence of the longest relaxation time, evaluated from dynamic shear rheology, compared favorably with the dependence of the rotational diffusion extracted from the zero-shear viscosity data according to the fuzzy cylinder model, whereas the relaxation times measured in a depolarized dynamic light scattering experiment did not correspond to the overall end-to end rotation of the chain. Concurrently, the relaxation time, which relates to the self-diffusion of the chain increased with concentration less rapidly than the viscosity of the solution, suggesting stronger entanglement effects in the rotational than in the translational motion of stiff chains.

Concluding we remark that this study demonstrates that careful assessment of all the parameters involved

in the fuzzy cylinder model description of the self-diffusion the zero shear viscosity and the rotational diffusion with independent experiments measuring directly D_s, D_R, and η_0 for different wormlike polymers is necessary and desirable; moreover further theoretical calculations of parameters such as $\beta_\perp$, β_R, and k_{HI} are needed in the framework of the fuzzy cylinder or the wormlike model.

References and Notes

(1) (a) Petekidis, G.; Vlassopoulos, D.; Fytas, G.; Rulkens, R.; Wegner, G. *Macromolecules* **1998**, *31*, 6129. (b) Petekidis, G.; Vlassopoulos, D.; Fytas, G.; Rulkens, R.; Wegner, G.; Fleischer, G. *Macromolecules* **1998**, *31*, 6139.

(2) Tinland, B.; Maret, G.; Rinaudo, M. *Macromolecules* **1990**, *23*, 596.

(3) Wang, L.; Garner, M. M.; Yu, H. *Macromolecules* **1991**, *24*, 2368.

(4) Bu, Z.; Russo, P. S.; Tipton, D. L.; Negulescu, I. I. *Macromolecules* **1994**, *27*, 6871.

(5) (a) Van Bruggen, M. P. B.; Lekkerkerker, H. N. W.; Dhont, J. K. G. *Phys. Rev. E* **1997**, *56*, 4394. (b) Van Bruggen, M. P. B.; Lekkerkerker, H. N. W.; Maret, G.; Dhont, J. K. G. *Phys. Rev. E* **1998**, *58*, 7668.

(6) Sato, T.; Takada, Y.; Teramoto, A. *Macromolecules* **1991**, *24*, 6220.

(7) Sato, T.; Teramoto, A. *Adv. Polym. Sci.* **1996**, *126*, 85.

(8) (a) Takada, Y.; Sato, T.; Teramoto, A. *Macromolecules* **1991**, *24*, 6215. (b) Sato, T.; Ohshima, A.; Teramoto, A. *Macromolecules* **1994**, *27*, 1477.

(9) Ohshima, A.; Kudo, H.; Sato, T.; Teramoto, A. *Macromolecules* **1995**, *28*, 6095.

(10) Ohshima, A.; Yamagata, A.; Sato, T.; Teramoto, A. *Macromolecules* **1999**, *32*, 8645.

(11) Altenberger, A. R.; Tirell, M. *J. Polym. Sci. Phys. Ed.* **1984**, *22*, 909.

(12) Russo, P. S. In *Dynamic Light Scattering. The Method and Some Applications*; Brown, W., Ed.; Clarendon Press: Oxford, U.K., 1993.

(13) Yamakawa, H.; Fujii, M. *Macromolecules* **1973**, *6*, 407.

(14) (a) Kratky, O.; Porod, G. *Recl. Trav. Chim.* **1949**, *68*, 1106. (b) Yamakawa, H. *Modern Theory of Polymer Solutions*; Harper and Row: New York, 1971.

(15) Doi, M.; Edwards, S. F. *The Theory of Polymer Dynamics*; Oxford University Press: New York, 1986.

(16) (a) Edwards, S. F.; Evans, K. E. *Trans. Faraday Soc.* **1982**, *78*, 113. (b) Edwards, S. F.; Vilgis, Th. *Phys. Scr.* **1986**, *T13*, 7.

(17) Teraoka, I.; Hayakawa, R. *J. Chem. Phys.* **1988**, *89*, 6989.

(18) Sato, T.; Teramoto, A. *Macromolecules* **1991**, *24*, 193.

(19) Doi, M. *J. Polym. Sci., Polym. Symp.* **1985**, *73*, 93. Odijk, T. *Macromolecules* **1984**, *17*, 502. Semenov, A. N. *J. Chem. Phys.* **1986**, *82*, 317.

(20) Cohen, M. H.; Turnbull, D. *J. Chem. Phys.* **1959**, *31*, 1164.

(21) Yoshizaki, T.; Yamakawa, H. *J. Chem. Phys.* **1984**, *81*, 982.

(22) Sato, T.; Ohshima, A.; Teramoto, A. *Macromolecules* **1998**, *31*, 3094.

(23) Yoshizaki, T.; Yamakawa, H. *J. Chem. Phys.* **1980**, *72*, 57.

(24) Petekidis, G.; Vlassopoulos, D.; Galda, P.; Rehahn, M.; Ballauff, M. *Macromolecules* **1996**, *29*, 8948.

(25) Karger, J.; Pfeiffer, H.; Heink, W. *Adv. Magn. Res.* **1988**, *12*, 1. Callaghan, P. T. *Principles of Nuclear Magnetic Resonance Microscopy*; Clarendon Press: Oxford, U.K. 1992.

(26) Karger, J.; Fleisher, G. *TRAC* **1994**, *13*, 145. Fleisher, G.; Fujara, *NMR Basic Princ. Prog.* **1994**, *30*, 159.

(27) Fleisher, G.; Rittig, F.; Stepanek, P.; Almdal, K.; Papadakis, C. M. *Macromolecules* **1999**, *32*, 1956.

(28) Macosko, C. W. *Rheology: Principles, measurements and applications*; VCH Publishers: New York, 1994.

(29) Baumgaertel, M.; Winter, H. H. *Rheol. Acta* **1989**, *28*, 511.

(30) Hoshikawa, H.; Saito, N.; Nagayama, K. *Polym. J.* **1975**, *7*, 79.

(31) Tagami, Y. *Macromolecules* **1969**, *2*, 8.

(32) Bitsanis, I.; Davis, H. T.; Tirrell, M. *Macromolecules* **1988**, *21*, 2824; **1990**, *23*, 1157.

(33) Petekidis, G.; Fytas, G.; Scherf, U.; Müllen, K.; Fleischer, G. *J. Polym. Sci., Polym. Phys. Ed.* **1999**, *37*, 2211.

(34) Ferry, J. D. *Viscoelastic Properties of Polymers*, 3rd ed.; John Wiley: New York, 1980.

(35) Vanhee, S.; Rulkens, R.; Lehmann, U.; Rosenauer, C.; Schulze, M.; Koehler, W.; Wegner, G. *Macromolecules* **1996**, *29*, 5136.

(36) Teraoka, I.; Ookubo, N.; Hayakawa, R. *Phys. Rev, Lett.* **1985**, *55*, 2712.

MA000976W